IEEE Access
Multidisciplinary ⋮ Rapid Review ⋮ Open Access Journal

Received 25 October 2022, accepted 13 November 2022, date of publication 17 November 2022, date of current version 9 December 2022.

Digital Object Identifier 10.1109/ACCESS.2022.3222762

RESEARCH ARTICLE

Robust Nonlinear Model Predictive Control for Ship Dynamic Positioning Using Laguerre Function

XIUHUI HOU, FANG DENG, HUALIN YANG, DUNJING YU, HANLIN ZHANG, AND BOYANG LI
College of Mechanical and Electrical Engineering, Qingdao University of Science and Technology, Qingdao 266061, China

Corresponding authors: Fang Deng (dengfhelen@163.com) and Hualin Yang (younghualin@163.com)

This work was supported in part by the National Natural Science Foundation of China under Grant 52101401; and in part by the Collaborative Innovation Center of Intelligent Green Manufacturing Technology and Equipment, Shandong, under Grant IGSD-2020-011.

ABSTRACT This paper is devoted to the issue of computationally efficient and robust nonlinear model predictive control (NMPC) for ship dynamic positioning (DP) systems subjected to input constraints and unknown environmental disturbances. The Laguerre functions, typically applied to the linear systems, are introduced to the constrained NMPC design of the nonlinear DP system to reduce the computational burden. The unscented Kalman filter is adopted to estimate the unknown disturbances and states; thus, the disturbance estimates are utilized as the cancellation signal to achieve robust offset-free control. Simulations of the proposed Laguerre function-based NMPC scheme are implemented and compared with the performance of typical Laguerre function-based linear model predictive control (LMPC) for the DP system. Simulation results well demonstrate the effectiveness, robustness and superiority of the proposed controller.

INDEX TERMS Laguerre functions, nonlinear model predictive control, input constraints, ship dynamic positioning.

I. INTRODUCTION

Marine vessels equipped with dynamic positioning (DP) system can automatically maintain the predefined position or trajectory through its thruster system. DP system has been extensively used in offshore operations, such as drilling, pipe laying, offloading and diving support [1], [2]. The control system is the core of the DP system. Grøvlen and Fossen firstly applied the nonlinear observer backstepping control to ship DP systems [3]. In recent years, many nonlinear advanced control methods, such as neural networks control [4], adaptive control [5], [6], and robust control [7], have been proposed in many literature. Considering that the thruster physically limits the control force in practical application, and the model predictive control (MPC) methods have the advantages of explicitly handling the physical constraints [8], [9], lots of attentions have been paid to MPC methods.

The associate editor coordinating the review of this manuscript and approving it for publication was Min Wang.

MPC refers to a multivariable control strategy that uses the predictive model to predict its future response and gain the control actions by online solving the constrained finite horizon optimal problem at each time step [10]. MPC methods have been extensively applied in different fields. In [11], [12], and [13], the linear MPC was implemented using the linearized state-space DP model based on the vessel parallel coordinate.

In the application of MPC, one of the challenges is its increased computational complexity for high-order systems [14]. In traditional MPC, a predefined optimization problem is online solved over the control horizon N_c, using the output over the predictive horizon N_P predicted based on the current states. By solving the optimization problem, the optimal control sequence over the future N_c time steps will be applied to obtain, and the first element of the sequence will be implemented in the system. To reduce the computational complexity, a shorter N_c with regard to N_P is generally adopted. Thus, the control increment signal over N_c is assumed to be zero. However, the ignored control increments

may change a little bit such that they are not zero, which may affect the MPC control performance [15], [16], [17]. Another method to increase the efficiency of online optimization is to parameterize the control signal with a set of orthogonal polynomial functions [18]. Laguerre functions are a set of typical orthogonal exponential basis functions. By using Laguerre functions, the decision variables of the MPC problem will change to the Laguerre coefficients, and the numbers will be much smaller [19]. Rossiter et al. and Wang designed MPC using Laguerre functions and verified its superiority in computational efficiency [19], [20]. Furthermore, since the exponential decay factors are included in the Laguerre network, the increments of control signals expressed by Laguerre functions will converge to zero. Recently, the application of Laguerre function-based MPC (Lag-MPC) have received significant attention in various areas, e.g., permanent magnet synchronous machine [21], stratospheric airship trajectory tracking [22], non-minimal state space model [18], vehicle automation [23], [24], and autonomous underwater vehicle [25].

It can be seen from the above literature that the standard Laguerre functions can only deal will the linear system, thus it is generally combined with the linear MPC. Considering that the DP system is nonlinear, the effect of linear MPC may not be satisfactory. Thus the nonlinear model predictive control (NMPC) was applied to DP, and its superior performance had been verified [26], [27]. To this end, it is essential to combine Laguerre functions with the NMPC to solve its computation complexity problem. Reference [28] introduced Laguerre polynomials into NMPC scheme to perform the air path control of a turbocharged gasoline engine, and verified that it is easier to fine-tune the NMPC scheme. However, current researches about Laguerre based MPC (or NMPC) in literature rarely consider the effect of disturbances. DP ships are disturbed by wind, waves and current forces, which will make the ship deviate from its required position. Thus, designing a robust nonlinear model predictive controller with anti-disturbances ability is crucial. Many robust control methods have been proposed to eliminate the effect of disturbances. In [27], two offset-free MPC strategies, including the target calculator formulation strategy and the delta input formulation strategy, were proposed. Both strategies utilized the UKF to estimate the unknown disturbances or the integrating input variables, and then took the estimates as inputs of the MPC algorithm to achieve the robust offset-free control. Comparing with the two strategies, the disturbance observer (DO) based control is regarded as one of the most promising approaches for disturbance rejection, and is relatively easy to solve and stabilize the system. To compensate for environmental disturbances, the disturbance observer has been proposed to estimate the unknown disturbances, and it has been combined with NMPC to directly remove the disturbance estimates as a cancellation signal [29], [30], [31], [32]. Yang et al. applied the disturbance observer-based NMPC (DO-NMPC) method to the DP system and verified its effectiveness, and robustness [30]. However, the implementation of DO-NMPC needs to assume that all the state variables are measurable or can be accurately estimated. Thus, considering the truth that only the position and heading can be measured for the DP system. The DP ship will oscillate around its equilibrium position due to the high-frequency first-order waves; the unscented Kalman filter (UKF) can be utilized to estimate the environmental disturbances and the unknown states and to filter out the wave-frequency motions [15]. Adopting the principle of disturbance observer, the disturbances estimated by UKF can be used as the cancellation signal to eliminate the effects of disturbances. The following points conclude the contributions of this work:

- To reduce the computational complexity, the Laguerre function is introduced into the NMPC design to parameterize the control signal, which can reduce the calculation amount of the controller, improve the efficiency of the online solution and accelerate the optimization process. In addition, this paper compares the proposed Laguerre function-based NMPC scheme with the typical Laguerre function-based linear model predictive control (LMPC). It proves that the nonlinear model predictive control method can improve the control accuracy of the DP system.
- The external disturbances are taken into account; they are eliminated by using of unscented Kalman filtering, thus the robustness of the novel Laguerre-based NMPC method is ensured.

The remainder of this paper is organized as follows. The Mathematical model and problem formulation of the DP system are described in Section II. In Section III, the NMPC using Laguerre functions is designed. Section IV presents simulation analysis and results discussions. The conclusions are described in Section V.

II. MATHEMATICAL MODEL AND PROBLEM FORMULATION

For DP surface vessels, the heave, roll and pitch motions in the vertical direction are neglected, and only the surge, sway and yaw in the horizontal plane are considered. To describe the motion of DP vessels, two reference frames are applied. One is the inertial earth-fixed frame $oxyz$, and another is the body-fixed frame $o_b x_b y_b z_b$ attached to the moving vessel. Refer to [33], for low-speed DP vessels with xz-symmetry, the nonlinear damping and the Coriolis-centripetal terms are neglected by accumulating these unmodeled dynamics into the bias disturbance terms. Thus, the mathematical model for DP vessels can be expressed as:

$$\dot{\boldsymbol{\eta}} = \boldsymbol{R}(\psi)\boldsymbol{v}, \tag{1}$$

$$\boldsymbol{M}\dot{\boldsymbol{v}} = -\boldsymbol{D}\boldsymbol{v} + \boldsymbol{\tau} + \boldsymbol{R}^T(\psi)\boldsymbol{d}, \tag{2}$$

where $\boldsymbol{\eta} = [x, y, \psi]^T$ is the low-frequency position and heading vector, $\boldsymbol{v} = [u, v, r]^T$ is the velocity vector, and $\boldsymbol{\eta}$ and $\boldsymbol{v}$ are described in the earth-fixed and body-fixed frame, respectively. $\boldsymbol{R}(\psi)$ is the transfer matrix between the earth-fixed frame and the body-fixed frame, $\boldsymbol{M}$ is the mass

matrix composed of rigid body mass and added mass, and $\boldsymbol{D}$ is the damping matrix. The matrices $\boldsymbol{R}(\psi)$, $\boldsymbol{M}$ and $\boldsymbol{D}$ are given as:

$$\boldsymbol{R}(\psi) = \begin{bmatrix} cos(\psi) & -sin(\psi) & 0 \\ sin(\psi) & cos(\psi) & 0 \\ 0 & 0 & 1 \end{bmatrix},$$

$$\boldsymbol{M} \begin{bmatrix} m - X_{\dot{u}} & 0 & 0 \\ 0 & m - Y_{\dot{v}} & mx_g - Y_{\dot{r}} \\ 0 & mx_g - Y_{\dot{r}} & I_z - N_{\dot{r}} \end{bmatrix},$$

$$\boldsymbol{D} = \begin{bmatrix} -X_u & 0 & 0 \\ 0 & -Y_v & -Y_r \\ 0 & -N_v & -N_r \end{bmatrix}$$

where m is the mass of the ship, I_z is the ship's inertia about z_b-axis, x_g is the x_b coordinate of the center of gravity, $X(\cdot)$, $Y(\cdot)$, $N(\cdot)$ are hydrodynamic derivatives.

In addition, $\boldsymbol{d} = [d_u, d_v, d_r]^T$ is the unknown disturbance vector described in the earth-fixed frame, including the environmental disturbance caused by second-order waves, ocean current, wind and model uncertainties caused by unmodeled nonlinear dynamics; $\boldsymbol{\tau} = [\tau_u, \tau_v, \tau_r]^T$ is the control input vector representing the generalized forces and moment generated by thrusters. The control input satisfies the thruster saturation constraints [34]:

$$\boldsymbol{\tau}_{min} \leq \boldsymbol{\tau} \leq \boldsymbol{\tau}_{max}, \tag{3}$$

$$\Delta\boldsymbol{\tau}_{min} \leq \Delta\boldsymbol{\tau} \leq \Delta\boldsymbol{\tau}_{max} \tag{4}$$

where $\boldsymbol{\tau}_{min}$ and $\boldsymbol{\tau}_{max}$ represent the minimum and maximum control forces and moment provided by the thruster system. $\Delta\boldsymbol{\tau}_{min}$ and $\Delta\boldsymbol{\tau}_{max}$ are the minimal and maximal input increments constraints, respectively.

Considering that only position (x, y) and the heading angle ψ can be measured, the state-space model for the DP system can be described as:

$$\dot{\boldsymbol{x}}(t) = \boldsymbol{A}(t)\boldsymbol{x} + \boldsymbol{B}(t)\boldsymbol{u} + \boldsymbol{B}_d(t)\boldsymbol{d}(t), \tag{5}$$

$$\boldsymbol{y}(t) = \boldsymbol{C}(t)\boldsymbol{x}, \tag{6}$$

where $\boldsymbol{x} = [\boldsymbol{\eta}^T, \boldsymbol{v}^T]^T$ is the state vector, $\boldsymbol{u} = \boldsymbol{\tau}$ is the control input vector, $\boldsymbol{y}(t)$ is the output vector, and

$$\boldsymbol{A}(\psi) = \begin{bmatrix} \boldsymbol{0}_{3\times3} & \boldsymbol{R}(\psi(t)) \\ \boldsymbol{0}_{3\times3} & -\boldsymbol{M}^{-1}\boldsymbol{D} \end{bmatrix}, \boldsymbol{B}(t) = \begin{bmatrix} \boldsymbol{0}_{3\times3} \\ -\boldsymbol{M}^{-1} \end{bmatrix},$$

$$\boldsymbol{B}_d(t) = \begin{bmatrix} \boldsymbol{0}_{3\times3} \\ \boldsymbol{M}^{-1}\boldsymbol{R}^T(\psi(t)) \end{bmatrix}, \boldsymbol{C}(t) = \begin{bmatrix} \boldsymbol{I}_{3\times3} & \boldsymbol{0}_{3\times3} \end{bmatrix}.$$

The aim of this paper is to operate the disturbed DP system (1) and (2) to follow the predefined reference trajectory in the presence of input saturation and unknown disturbances. In specific, for the demanded reference trajectory $\boldsymbol{\eta}_r(t) = [x_r(t), y_r(t), \psi_r(t)]^T$, the control input shall be determined to achieve:

$$\lim_{t\to\infty} \|\boldsymbol{y}(t) - \boldsymbol{\eta}_r(t)\| = 0 \tag{7}$$

III. CONTROL FORMULATION

In this section, by representing the NMPC optimization problem with Laguerre functions, an improved nonlinear predictive control scheme is proposed to realize the control mode of setpoint regulation and trajectory tracking for DP systems. The Laguerre functions are used to parameterize the control sequence. It is possible to reduce the number of constraints in the prediction horizon; thus, the number of parameters that exist in each optimization step will be reduced, and consequently increase the computational efficiency. Furthermore, the UKF estimator is adopted to estimate the unknown disturbances and states. Herein, based on the principle of disturbance observer, the disturbance estimates can be used as a cancellation signal to eliminate the effects of disturbances. The control scheme of the proposed robust Laguerre-based NMPC with UKF estimator is shown in Figure 1.

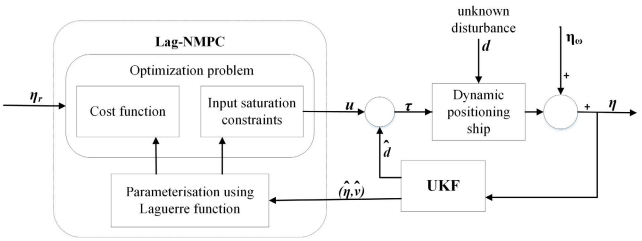

FIGURE 1. Control scheme of Laguerre-based NMPC with UKF estimator.

A. DISCRETE-TIME NMPC SCHEME

Based on the idea of feedforward control, the influence of interference is directly eliminated in the control signal. Thus, the controller is designed according to the determined nominal model of the DP system, which is:

$$\dot{\boldsymbol{x}}(t) = \boldsymbol{A}(t)\boldsymbol{x} + \boldsymbol{B}(t)\boldsymbol{u}, \tag{8}$$

$$\boldsymbol{y}(t) = \boldsymbol{C}(t)\boldsymbol{x} \tag{9}$$

In general, MPC is designed using the discrete-time state-space model. Hence, the DP models (8) and (9) are discretized at the current operating point using the sampling time T_s as follows:

$$\boldsymbol{x}(k+1) = \boldsymbol{A}(k)\boldsymbol{x}(k) + \boldsymbol{B}(k)\boldsymbol{u}(k), \tag{10}$$

$$\boldsymbol{y}(k) = \boldsymbol{C}(k)\boldsymbol{x}(k), \tag{11}$$

where $k = \frac{t}{T_s}$, $\boldsymbol{x}(k) = \left[\boldsymbol{\eta}(k)^T, \boldsymbol{v}(k)^T\right]^T$ indicates the state variable vector of the plant at the sample time k, $\boldsymbol{u}(k) = [\tau_u(k), \tau_v(k), \tau_r(k)]^T$ is the control signal, $\boldsymbol{y}(k) = [x(k), y(k), \psi(k)]^T$ is the system output, respectively.

To remove steady state errors, it is meaningful to embed integrators into (10) to deal with the control increment $\Delta\boldsymbol{u}(k) = \boldsymbol{u}(k) - \boldsymbol{u}(k-1)$. Supposing that the DP system has n_u inputs and n_y outputs and the number of states is equal to n_x, defining the new state variable vector as $\boldsymbol{x}_a(k) = \left[\Delta\boldsymbol{x}(k)^T \ \boldsymbol{y}(k)^T\right]^T$, then the augment state-space model with

an integrator is established as:

$$\overbrace{\begin{bmatrix}\Delta \boldsymbol{x}(k+1)\\ \boldsymbol{y}(k+1)\end{bmatrix}}^{\boldsymbol{x}_a(k+1)} = \overbrace{\begin{bmatrix}A_k & 0^T_{n_y\times n_x}\\ CA_k & I_{n_y\times n_y}\end{bmatrix}}^{\boldsymbol{A}_a}\overbrace{\begin{bmatrix}\Delta \boldsymbol{x}(k)\\ \boldsymbol{y}(k)\end{bmatrix}}^{\boldsymbol{x}_a(k)} + \overbrace{\begin{bmatrix}B_k\\ CB_k\end{bmatrix}}^{\boldsymbol{B}_a}\Delta \boldsymbol{u}(k) \tag{12}$$

$$\boldsymbol{y}(k) = \overbrace{\begin{bmatrix}0_{n_y\times n_x} & I_{n_y\times n_y}\end{bmatrix}}^{\boldsymbol{C}_a}\overbrace{\begin{bmatrix}\Delta \boldsymbol{x}(k)\\ \boldsymbol{y}(k)\end{bmatrix}}^{\boldsymbol{x}_a(k)} \tag{13}$$

where $\Delta \boldsymbol{x}(k)$ is the state increment and $\Delta \boldsymbol{x}(k) = \boldsymbol{x}(k) - \boldsymbol{x}(k-1)$, $\boldsymbol{A}_a$, $\boldsymbol{B}_a$ and $\boldsymbol{C}_a$ are corresponding augmented model state-space matrices. Given N_c and N_P the control and the prediction horizons, respectively, the NMPC optimization problem can be defined as:

$$\begin{aligned}
\min_{\Delta U} J = &\sum_{i=1}^{N_P}\left\|(\boldsymbol{\eta}_r(k) - \boldsymbol{y}(k+i))^T\right\|^2_{\boldsymbol{w}_y}\\
&+\sum_{i=0}^{N_c-1}\|\Delta \boldsymbol{u}(k+i)\|^2_{\boldsymbol{w}_{\Delta u}}\\
s.t.\quad &\boldsymbol{x}_a(k+i) = \boldsymbol{A}_a\boldsymbol{x}_a(k+i) + \boldsymbol{B}_a\Delta \boldsymbol{u}(k+i),\\
&i = 1, 2, \ldots, N_P,\\
&\boldsymbol{y}(k+i) = \boldsymbol{C}_a\boldsymbol{x}_a(k+i),\\
&i = 1, 2, \ldots, N_P,\\
&\Delta \boldsymbol{u}_{\min} \le \Delta \boldsymbol{u}(k+j) \le \Delta \boldsymbol{u}_{\max},\\
&j = 1, 2, \ldots, N_c - 1\\
&\boldsymbol{u}_{\min} \le \boldsymbol{u}(k+j) \le \boldsymbol{u}_{\max},\\
&j = 1, 2, \ldots, N_c - 1.
\end{aligned} \tag{14}$$

where $\boldsymbol{x}(k+i)$, $\boldsymbol{y}(k+i)$ and $\Delta \boldsymbol{u}(k+i)$ represent the ith step future predictive state, output and control increment variables of the current instant k, respectively, they can be computed based on the current state $\boldsymbol{x}(k)$; $\Delta U = [\Delta \boldsymbol{u}(k) \Delta \boldsymbol{u}(k+1) \quad \cdots \quad \Delta \boldsymbol{u}(k+N_c-1)]^T$ is the future control sequence to be determined by solving the optimization problem; $\boldsymbol{w}_y$ and $\boldsymbol{w}_{\Delta u}$ are weights for the system outputs and control increments, respectively.

Remark 1: The discretized model (10) is nonlinear, and however, considering the DP ship's sailing state changes slowly, it is presumed that state matrix $\boldsymbol{A}(k)$, $\boldsymbol{B}(k)$, and the augmented matrix $\boldsymbol{A}_a(k)$, $\boldsymbol{B}_a(k)$ remain unchanged in the prediction horizon N_P. Thus, the future prediction output $\boldsymbol{y}(k+i)$ for $i = 1, 2, \ldots, N_P$ can be calculated as a linear model.

Remark 2: To reduce the computational complexity, the classical NMPC often lets $N_c < N_P$, and the NMPC optimizer only gives the optimal solution within the horizon N_c, while the control increments over N_c are assumed to be zero, that is $\Delta \boldsymbol{u}(k+i) = 0$ when $i = N_c, N_c+1, \ldots N_P$. However, the ignored control increments may have a small change but are not zero, which may influence the MPC control effect. Considering that the control signal $\Delta \boldsymbol{u}(k+i)$ can be parameterized using a set of orthogonal polynomial functions, i.e., the typical orthogonal basis functions named Laguerre functions, the NMPC optimization problem is going to be expressed using Laguerre functions to increase the computational efficiency.

B. PARAMETERISATION USING DISCRETE-TIME LAGUERRE FUNCTIONS

Laguerre functions are a set of orthonormal basis functions which can be adopted to reconstruct the NMPC online optimization problem. The z-transform of the discrete-time Laguerre networks can be written as:

$$\Gamma_{k+1}(z, a) = \Gamma_k(z, a)\left(\frac{z^{-1} - a}{1 - az^{-1}}\right), k = 1, 2, \ldots, N-1 \tag{15}$$

with $\Gamma_1(z, a) = \frac{\sqrt{1-a^2}}{1-az^{-1}}$,where N is the number of terms, a is the scale factor representing the pole of the Laguerre functions. For stability, it is necessary to set $0 \le a < 1$. Let $l_1(k), l_2(k), \cdots, l_N(k)$ represent the inverse z-transform of $\Gamma_1(z, a), \Gamma_2(z, a), \cdots, \Gamma_N(z, a)$, respectively, the set of discrete-time Laguerre function can be rewritten as a vector form of $L(k) = [\, l_1(k)\ l_2(k) \cdots l_N(k)\,]^T$. Considering Laguerre networks (15), it is derived that $L(k)$ satisfies the following relation:

$$L(k+1) = A_l L(k) \tag{16}$$

where A_l is a $N \times N$ matrix about parameters a and $\beta = 1 - a^2$. Its definition is

$$A_l = \begin{bmatrix} a & 0 & 0 & \cdots & 0\\ \beta & a & 0 & \cdots & 0\\ -a\beta & \beta & 0 & \cdots & 0\\ a^2\beta & -a\beta & \ddots & \ddots & \vdots\\ \vdots & \vdots & \ddots & a & 0\\ (-1)^{N-2}a^{N-2}\beta & (-1)^{N-3}a^{N-3}\beta & \cdots & \beta & a \end{bmatrix}$$

and

$$L(0)^T = \sqrt{\beta}[\,1\ -a\ a^2\ -a^3\ \cdots\ (-1)^{N-1}a^{N-1}\,] \tag{17}$$

It is obvious that when $a = 0$, the Laguerre functions reduce to a set of pulses, which becomes equivalent to the traditional MPC method. Thus, it is important to set $a > 0$ to achieve performance improvements. The orthonormal property of Laguerre functions can be shown as follows:

$$\sum_{k=0}^{\infty} l_i(k) l_j(k) \begin{cases} =0 & for\ i \ne j\\ =1 & for\ \ i = j \end{cases} \tag{18}$$

Considering the single-input system, the control increments $\Delta u(k)$, $\Delta u(k+1), \ldots, \Delta u(k+N_c-1)$ at time k are equivalent to the impulse response of a stable dynamic system. Thus, a set of Laguerre functions along with a set of Laguerre coefficients can be applied to describe the dynamic responses of the control increment as:

$$\Delta u(k+i) = \sum_{j=1}^{N} c_j(k) l_j(i) \tag{19}$$

where k is the initial time of the moving horizon, i is the future sample instant, $c_j(k), j = 1, 2, \cdots, N$ are the Laguerre coefficients for corresponding Laguerre function $l_1(i), l_2(i), \cdots, l_N(i)$. Eq.(19) shows that the number of terms N instead of the control horizon N_c is used to describe the complexity of control increment. To reduce the compute complexity, a larger value of scale factor a with a smaller number of terms N, i.e., $N < N_c$, can be selected to achieve the performance with a long control horizon.

Further defining the Laguerre coefficient vector as $\boldsymbol{\gamma}(i)= [c_1(i) \quad c_2(i) \quad \cdots \quad c_N(i)]^T$, Eq.(19) can be rewritten as:

$$\Delta u(k+i) = L(i)^T \boldsymbol{\gamma}(i) \tag{20}$$

For the multi-input system with an input number of n_u, each element in the control trajectory will be an $1 \times n_u$ vector that $\Delta \boldsymbol{u}(k)= \left[\Delta u_1(k) \quad \Delta u_2(k) \quad \cdots \quad \Delta u_{n_u}(k)\right]^T$. By assigning a specific scaling factor a_p and number N_p for the pth control signal $\Delta u_p(k)$, we can describe the particular control input as $\Delta u_p(i) = \boldsymbol{L}_p(i)^T \boldsymbol{\gamma}_p(i)$ with $\boldsymbol{L}_p(i) = [\, l_{p1}(i)\, l_{p2}(i) \cdots l_{pN}(i)\,]^T$, $\boldsymbol{\gamma}_p(i) = \left[\, c_{p1}(i)\, c_{p2}(i) \cdots c_{pN}(i)\,\right]^T$, where $\boldsymbol{L}_p(i)$ and $\boldsymbol{\gamma}_p(i)$ are the individual Laguerre function and efficient vector for the pth control input, respectively. Thus, for the multi-input system, the control signal $\Delta \boldsymbol{u}(i)$ can be expressed using the Laguerre network as:

$$\begin{aligned}\Delta \boldsymbol{u}(k+i) &= \begin{bmatrix} \boldsymbol{L}_1(i) & \boldsymbol{o}_1 & \cdots & \boldsymbol{o}_1 \\ \boldsymbol{o}_2 & \boldsymbol{L}_2(i) & \cdots & \boldsymbol{o}_2 \\ \vdots & \vdots & \ddots & \vdots \\ \boldsymbol{o}_{n_u} & \boldsymbol{o}_{n_u} & \cdots & \boldsymbol{L}_{n_u}(i) \end{bmatrix}^T \boldsymbol{\gamma}(i) \\ &= \boldsymbol{L}(i)^T \boldsymbol{\gamma}(i) \end{aligned} \tag{21}$$

with $\boldsymbol{\gamma}(i) = [\, \boldsymbol{\gamma}_1(i)^T \; \boldsymbol{\gamma}_2(i)^T \; \cdots \; \boldsymbol{\gamma}_{n_u}(i)^T \,]^T$, where $\boldsymbol{o}_p, p = 1, 2, \cdots, n_u$ represents a zero block column vector with identical dimension to $L_p(i)$.

Remark 3: In the design of the model predictive controller, the Laguerre function is used to represent the future control increment trajectory of the system. Noting that for LMPC and NMPC, the Laguerre function have the same representations for the control increment trajectory. However, since the LMPC is implemented using the linear dynamic model derived by the vessel parallel coordinate system, the control accuracy will be affected. While the NMPC adopts the nonlinear dynamic model and linearizes the nonlinear model near the operating point at each time step when solving the nonlinear optimization problem, which will improve the control performance of DP.

C. LAGUERRE FUNCTION-BASED NMPC WITH INPUT SATURATION CONSTRAINTS

Applying the Laguerre network expression Eq.(21) to the augmented state-space model (12) and (13), the ith step predicted state variables $\boldsymbol{x}_a(k+i)$ and the output variable $\boldsymbol{y}(k+i)$ within the prediction horizon at sample time k can be expressed as:

$$\boldsymbol{x}_a(k+i) = \boldsymbol{A}_a^i \boldsymbol{x}_a(k) + \sum_{j=0}^{i-1} \boldsymbol{A}_a^{i-j-1} \boldsymbol{B}_a \boldsymbol{L}(j)^T \boldsymbol{\gamma}, \tag{22}$$

$$\boldsymbol{y}(k+i) = \boldsymbol{C}_a \boldsymbol{A}_a^i \boldsymbol{x}_a(k) + \boldsymbol{C}_a \sum_{j=0}^{i-1} \boldsymbol{A}_a^{i-j-1} \boldsymbol{B}_a \boldsymbol{L}(j)^T \boldsymbol{\gamma} \tag{23}$$

Substituting (23) into the NMPC optimization problem defined in (14), the Laguerre function-based NMPC optimizer for the minimization of the errors between the reference signal and the output signal could be reformulated using the Laguerre coefficient vector $\boldsymbol{\gamma}$:

$$\begin{aligned} J = \boldsymbol{\gamma}^T &\left(\sum_{i=1}^{N_p} \phi(i) \boldsymbol{Q}_L \phi(i)^T + \boldsymbol{R}_L \right) \boldsymbol{\gamma} \\ &+ 2\boldsymbol{\gamma}^T \left(\sum_{i=1}^{N_p} \phi(i) \boldsymbol{Q}_L A_a^i \right) \boldsymbol{x}_f(k) \end{aligned} \tag{24}$$

where the data matrix $\phi(i)^T = \sum_{j=0}^{i-1} \boldsymbol{A}_a^{i-j-1} \boldsymbol{B}_a \boldsymbol{L}(j)^T$, the new state $\boldsymbol{x}_f(k) = \left[\Delta \boldsymbol{x}(k)^T \boldsymbol{y}(k) - \boldsymbol{r}(k)\right]^T$, the weighting matrix $\boldsymbol{Q}_L = \boldsymbol{C}_a^T \boldsymbol{C}_a$ is used for the purpose of minimizing the reference tracking errors, $\boldsymbol{R}_L$ is a diagonal matrix with dimension equal to the dimension of $\boldsymbol{\gamma}$.

It can be observed from (24) that the decision variables have been changed from the control increment $\Delta \boldsymbol{u}$ to the Laguerre coefficient $\boldsymbol{\gamma}$. Thus, the control constraint of the control increment signal $\Delta \boldsymbol{u}(i)$ and the control signal $\boldsymbol{u}(i)$ shall be expressed as an inequality about $\boldsymbol{\gamma}$. Noting that the increment of the control signal is $u\,(i) = \sum_{j=0}^{i-1} \Delta\, u\,(j)$ and the Laguerre expression (22), the control constraints of the future sample time k can be expressed as (25) and (26), shown at the bottom of the next page, where $\boldsymbol{u}(k-1)$ is the control signal of $k-1$, $\boldsymbol{o}_p^T$ is the zero row vector. In practical, the constraints (25) and (26) need to be transferred into a standard inequality expression of $\boldsymbol{\gamma}$, which can be written as:

$$\overbrace{\begin{bmatrix} G_{\Delta U} \\ -G_{\Delta U} \\ G_U \\ -G_U \end{bmatrix}}^{G} \boldsymbol{\gamma} \leq \overbrace{\begin{bmatrix} \Delta U^{\max} \\ -\Delta U^{\min} \\ U^{\max} - U^{k-1} \\ -U^{\min} + U^{k-1} \end{bmatrix}}^{\sigma} \tag{27}$$

where $U^{k-1} = \left[u_1(k-1) \;\; u_2(k-1) \;\; \ldots \;\; u_q(k-1)\right]^T$ is the vector containing the previous u for each input, $\Delta U^{\min} = \left[\Delta u_1^{\min}(k-1) \;\; \Delta u_2^{\min}(k-1) \;\; \ldots \;\; \Delta u_q^{\min}(k-1)\right]^T$, $U^{\min} = \left[u_1^{\min}(k-1)\; u_2^{\min}(k-1) \;\ldots\; u_q^{\min}(k-1)\right]^T$, and $\Delta U^{\max} = [\Delta u_1^{\max}(k-1)\; \Delta u_2^{\max}(k-1) \;\ldots \Delta u_q^{\max}(k-1)]^T$, $U^{\max} = \left[u_1^{\max}(k-1)\; u_2^{\max}(k-1) \;\ldots\; u_q^{\max}(k-1)\right]^T$ are the minimum and maximum values for each input, respectively. $G_{\Delta U}$ and G_U are control increment and control signal constraint

matrices, respectively. It can be computed as:

$$G_{\Delta U}=\begin{bmatrix} P(1) \\ P(2) \\ \vdots \\ P(N_{sum}) \end{bmatrix},\ G_U=\begin{bmatrix} P(1) \\ P(1)+P(2) \\ \vdots \\ \sum_{i=1}^{N_{sum}} P(q) \end{bmatrix}$$

where $P(q),\ q=1,2,\ldots,N_{sum}$ is the block matrix consisting of Laguerre functions, it can be computed by:

$$P(k)=\begin{bmatrix} (A_{l_1}^{k-1}L_1(0))^T & o_2^T & \cdots & o_{n_u}^T \\ o_1^T & (A_{l_2}^{k-1}L_2(0))^T & \cdots & o_{n_u}^T \\ \vdots & \vdots & \ddots & \vdots \\ o_1^T & o_2^T & \cdots & (A_{l_{n_u}}^{k-1}L_{n_u}(0))^T \end{bmatrix},$$

where $o_p^T p = 1,2\ldots,n_u$ are all zero row vectors with dimensions $L_{n_u}(0)^T$. The $N_{sum}=N_1+N_2+\ldots+N_{n_u}$ is equal to the sum of the order of the Laguerre network, and N_{sum} is also the number of future samples for constraints to be imposed, which is used to predict the future control trajectory. Further defining $\Omega=\sum_{i=1}^{N_p}\phi(i)\boldsymbol{Q}_L\phi(i)^T+\boldsymbol{R}_L$ and $\Psi=\sum_{i=1}^{N_p}\phi(i)\boldsymbol{Q}_L\boldsymbol{A}_a^i$, the Lag-NMPC optimization problem can be expressed as:

$$\begin{aligned} &\min J=\boldsymbol{\gamma}^T\Omega\boldsymbol{\gamma}+2(\Psi\boldsymbol{x}_f(k))^T\boldsymbol{\gamma} \\ &s.t.\ \boldsymbol{G}\boldsymbol{\gamma}\le\boldsymbol{\sigma} \end{aligned} \tag{28}$$

where $\boldsymbol{G}$ and $\boldsymbol{\sigma}$ are constraints matrix of $\boldsymbol{\gamma}$, they are computed according to (27). Thus, the Lag-NMPC optimization problem (29) is a quadratic programming problem solved by the active set or interior point method. Given that the optimal Laguerre coefficient solved out is $\boldsymbol{\gamma}^*(k)$, then the optimal control increment at the current time k can be determined by:

$$\Delta\boldsymbol{u}^*(k+i)=\boldsymbol{L}(i)^T\boldsymbol{\gamma}^*(i) \tag{29}$$

D. DISTURBANCE ESTIMATION AND WAVE FILTERING USING UKF

A tracking error will occur if disturbances caused by the environment interfere and model uncertainties are not considered in the controller design. Since the disturbances are usually priori unknown, it is necessary to estimate the disturbance. Furthermore, for the DP system, it is generally considered that only the ship position and heading can be measured, and the other states, such as ship velocities, can not be measured. The first-order wave force will cause the vessel to produce high-frequency oscillation (wave frequency motion) with the same frequency as the wave. However, from the point of reducing energy consumption and the wear and tear of the thrusters, there is not necessary for the controller to respond to them. Hence, the wave-frequency motion needs to be filtered out by wave filtering. To this end, the UKF method is adopted herein to obtain the unknown disturbance estimates and ship velocities and to filter out the wave-frequency motions simultaneously. Motivated by the principle of disturbance observer control for disturbance rejection, the estimated disturbances will be fed back as a cancellation signal to eliminate the tracking errors and achieve offset-free control directly. To achieve the objective of unknown disturbance estimation and wave filtering, the DP observer model is established as follows:

$$\dot{\boldsymbol{\xi}} = \boldsymbol{A}_\omega\xi+\boldsymbol{E}_\omega\boldsymbol{w}_1, \tag{30}$$
$$\dot{\boldsymbol{\eta}} = \boldsymbol{R}(\psi)\boldsymbol{v}, \tag{31}$$
$$\dot{\boldsymbol{d}} = -T_d^{-1}\boldsymbol{d}+\boldsymbol{w}_2, \tag{32}$$
$$\boldsymbol{M}\dot{\boldsymbol{v}} = -\boldsymbol{D}\boldsymbol{v}+\boldsymbol{\tau}+\boldsymbol{R}(\psi)\boldsymbol{d}+\boldsymbol{w}_3, \tag{33}$$
$$\boldsymbol{y} = \boldsymbol{\eta}+\boldsymbol{\eta}_\omega+\boldsymbol{\varsigma} \tag{34}$$

where $\boldsymbol{\eta}_\omega=\boldsymbol{C}_\omega\boldsymbol{\xi}$ is the wave-induced high-frequency motion with state vectors $\boldsymbol{\xi}\in\mathbb{R}^6$, $\boldsymbol{A}_\omega\in\mathbb{R}^{6\times6}$ and $\boldsymbol{E}_\omega\in\mathbb{R}^{6\times3}$, which are constant sea state matrices, $\boldsymbol{w}_i(i=1,2,3)$ are zero-mean Gaussian noise vectors, and $\boldsymbol{\varsigma}\in\mathbb{R}^3$ is the measurement noise vector, $\boldsymbol{d}\in\mathbb{R}^3$ is the disturbance vector. The observer model (30)-(34) can be described in the form of state-space as follows:

$$\dot{\boldsymbol{\chi}} = \boldsymbol{A}_o\dot{\boldsymbol{\chi}}+\boldsymbol{B}_o\boldsymbol{u}+\boldsymbol{E}\boldsymbol{w}, \tag{35}$$
$$\boldsymbol{y} = \boldsymbol{H}\dot{\boldsymbol{\chi}}+\boldsymbol{\varsigma} \tag{36}$$

where $\boldsymbol{\chi}=\left[\boldsymbol{\xi}^T,\boldsymbol{\eta}^T,\boldsymbol{d}^T,\boldsymbol{v}^T\right]^T\in\mathbb{R}^{15}$ is a 15th-order state vector, $\boldsymbol{w}=\left[\boldsymbol{w}_1^T,\boldsymbol{w}_2^T,\boldsymbol{w}_3^T\right]^T\in\mathbb{R}^9$ is the process noise vector. In order to carry out UKF state estimation and filtering, (35) and (36) need to be rewritten as the following standard discrete-time state-space form:

$$\dot{\boldsymbol{\chi}}(k+1) = \boldsymbol{A}_{od}\boldsymbol{\chi}(k)+\boldsymbol{B}_{od}\boldsymbol{u}(k)+\boldsymbol{E}_d\boldsymbol{w}(k), \tag{37}$$
$$\boldsymbol{y}(k) = \boldsymbol{H}\boldsymbol{\chi}(k)+\boldsymbol{\varsigma}(k) \tag{38}$$

where $\boldsymbol{\chi}(k)\in\mathbb{R}^{15}$ is the observation state vector, $\boldsymbol{w}(k)$ and $\boldsymbol{\varsigma}(k)$ are Gaussian zero-mean process noise of process. The state observation and filtering of the DP vessels are designed

$$\Delta\boldsymbol{u}_{\min}\le\boldsymbol{L}(k+i)^T\boldsymbol{\gamma}\le\Delta\boldsymbol{u}_{\max} \tag{25}$$

$$\begin{aligned} \boldsymbol{u}_{\min}\le&\begin{bmatrix} \sum_{j=0}^{i-1}\boldsymbol{L}_1(k)^T & \boldsymbol{o}_2^T & \cdots & \boldsymbol{o}_{n_u}^T \\ \boldsymbol{o}_1^T & \sum_{j=0}^{i-1}\boldsymbol{L}_2(k)^T & \cdots & \boldsymbol{o}_{n_u}^T \\ \vdots & \vdots & \ddots & \vdots \\ \boldsymbol{o}_1^T & \boldsymbol{o}_2^T & \cdots & \sum_{j=0}^{i-1}\boldsymbol{L}_{n_u}(k)^T \end{bmatrix}\boldsymbol{\gamma}+\boldsymbol{u}(k-1) \\ \le&\boldsymbol{u}_{\max} \end{aligned} \tag{26}$$

as:

$$\hat{\boldsymbol{\chi}}(k+1) = \boldsymbol{A}_{od}\boldsymbol{\chi}(k) + \boldsymbol{B}_{od}\boldsymbol{u}(k) + \boldsymbol{K}_{od}(\boldsymbol{y}(k) - \boldsymbol{H}\hat{\boldsymbol{\chi}}(k)) \tag{39}$$

where $\boldsymbol{K}_{od}$ is the observer gain matrix which can be determined using UKF method. Given the covariance matrix of the process and measurement noises are $\boldsymbol{Q}$ and $\boldsymbol{R}$, respectively, initializing mean and covariance as $\hat{\boldsymbol{\chi}}(0)$ and $\boldsymbol{P}(0)$, then the matrix composed of $2n+1$ sigma points can be computed as:

$$\begin{aligned}\boldsymbol{\mu}(k-1) = \Big[&\hat{\boldsymbol{\chi}}(k-1),\ \hat{\boldsymbol{\chi}}(k-1) + \sqrt{(n+\lambda)\boldsymbol{P}(k-1)},\\ &\hat{\boldsymbol{\chi}}(k-1) \quad - \sqrt{(n+\lambda)\boldsymbol{P}(k-1)}\Big]\end{aligned} \tag{40}$$

thus the transformation points of the process and measurement model for each sigma point can be obtained as:

$$\begin{aligned}\boldsymbol{X}^i(k) &= \boldsymbol{A}_{od}\boldsymbol{\mu}^i(k-1) + \boldsymbol{B}_{od}\boldsymbol{u}(k-1),\\ &\quad i = 0, 1, \ldots, 2n,\end{aligned} \tag{41}$$

$$\boldsymbol{Y}^i(k) = \boldsymbol{H}\boldsymbol{\mu}^i(k-1), i = 0, 1, \ldots, 2n, \tag{42}$$

Based on the Kalman filter principle, the transformed points are used to calculate the predicted mean $\hat{\boldsymbol{\chi}}^-(k-1)$ and its associated covariance $\boldsymbol{P}^-(k-1)$, the predicted measurement $\hat{\boldsymbol{y}}^-(k-1)$, the innovation covariance $\boldsymbol{P}^{yy}(k)$ and the cross-covariance $\boldsymbol{P}^{xy}(k)$. And then, the state and covariance estimates can be computed as:

$$\hat{\boldsymbol{\chi}}(k) = \hat{\boldsymbol{\chi}}^-(k) + \boldsymbol{K}_{od}(\hat{\boldsymbol{y}}(k) - \hat{\boldsymbol{y}}^-(k)), \tag{43}$$

$$\boldsymbol{P}(k) = \boldsymbol{P}^-(k) - \boldsymbol{K}_{od}\boldsymbol{P}^{yy}(k)\boldsymbol{K}^T(k) \tag{44}$$

where the Kalman gain $\boldsymbol{K}_{od}$ is calculated by:

$$\boldsymbol{K}_{od} = \boldsymbol{P}^{xy}(k)(\boldsymbol{P}^{yy}(k))^{-1} \tag{45}$$

For more details on UKF, see [35]. Therefore, when designing the nonlinear model predictive controller, it is only necessary to replace the system state with the state estimation value to realize the output feedback control. In the solving process of nonlinear model predictive control constrained optimization problem (14), the current state variable $\boldsymbol{x}(k)$ is replaced by its estimated value $\hat{\boldsymbol{x}}(k)$.

E. IMPLEMENTATION OF ROBUST LAG-NMPC

The Lag-NMPC optimization problem (14) is designed based on the nonlinear state-space DP model (5) and (6) in the presence of environmental disturbance. Disturbance estimates $\hat{\boldsymbol{d}}(t)$ can be obtained using UKF state observation and filtering (39). We can acquire the optimal control law $\boldsymbol{\tau}(k) = \Delta\boldsymbol{u}^*(k) + \boldsymbol{u}(k-1) - \hat{\boldsymbol{d}}(k)$ by taking the disturbance estimates $\hat{\boldsymbol{d}}(t)$ as a feedback signal in the outer loop control. Figure 2 shows the workflow of the proposed robust lag NMPC with UKF.

IV. SIMULATION ANALYSIS AND RESULTS DISCUSSIONS

In order to verify the performance of the proposed Lag-NMPC strategy, the reference tracking performance of Cybership II (CSII) under saturation constraints and unknown disturbances is simulated. CSII ship is a 1:70 scale model of a supply ship, and its prior identified dynamic parameters for CSII are shown in Table 1. The minimal and maximal input constraints are $\boldsymbol{\tau}_{min}=[-2.0\,N, -2.0\,N, -1.5\,N\cdot m]^T$ and $\boldsymbol{\tau}_{max}=[2.0\,N, 2.0\,N, 1.5\,N\cdot m]^T$, respectively. The input increments constraints are set as $\Delta\boldsymbol{\tau}_{min}=[-1.0\,N, -0.5\,N, -0.5\,N\cdot m]^T$ and $\Delta\boldsymbol{\tau}_{max}=[1.0\,N, 0.5\,N, 0.5\,N\cdot m]^T$, respectively. A computer with AMD Ryzen 7 3700X 8-Core Processor (3593 MHz) CPU and 16.00 GB (3200 MHz) memory is used to simulate and verify the designed controller.

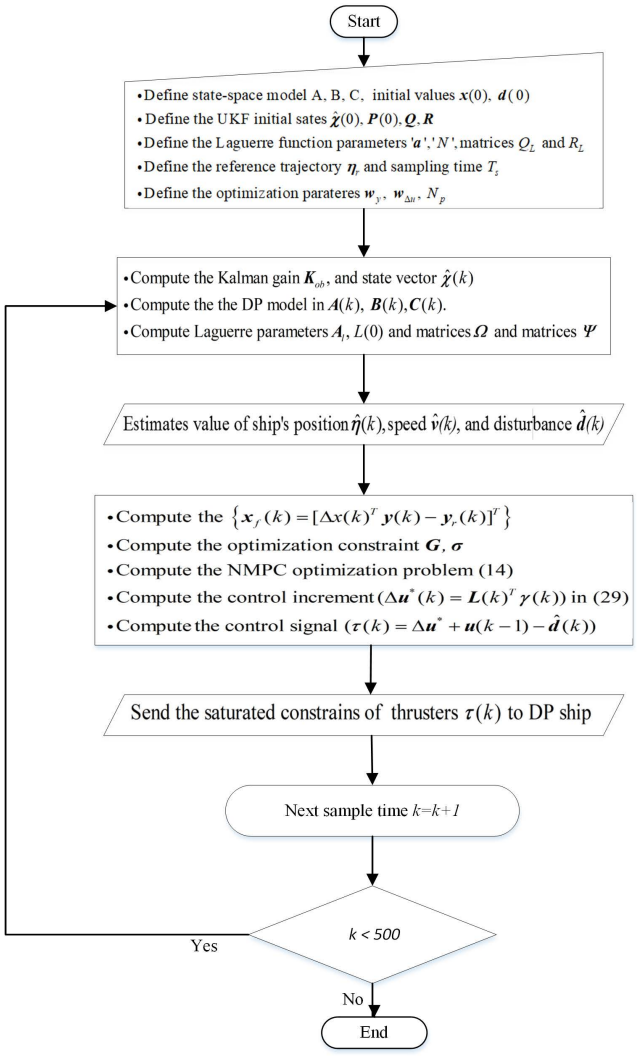

FIGURE 2. Flow chart of the offset-free Lag-NMPC scheme.

TABLE 1. CSII ship parameters [35].

Parameter	Value	Unit	Parameter	Value	Unit
m	23.8	kg	$N_{\dot{r}}$	-1.0	kg· m^2
I_z	1.76	kg· m^2	X_u	-2	kg/s
x_g	0.046	m	Y_v	-7	kg/s
$X_{\dot{u}}$	-2.0	kg	Y_r	-0.1	kg· m/s
$Y_{\dot{v}}$	-10.0	kg	N_v	-1.0	kg· m/s
$Y_{\dot{r}}$	-0.0	kg· m	N_r	-0.5	kg· m^2 /s

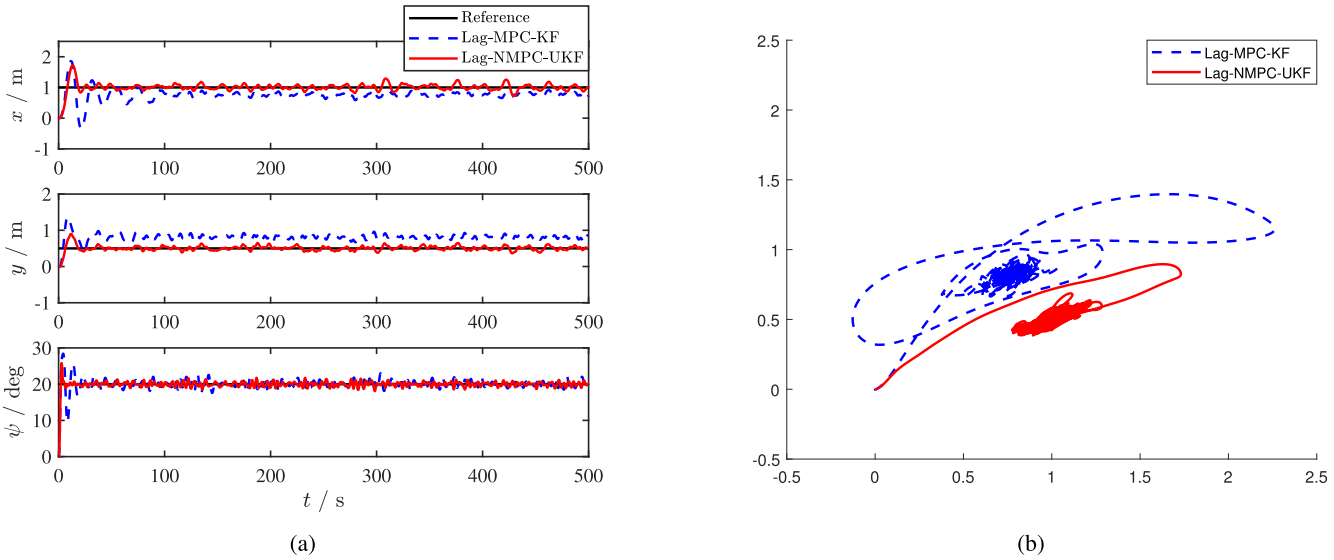

FIGURE 3. The simulation results of scenario 1 (setpoint regulation): (a) North-east position and heading (x, y, ψ); (b)Ship's horizontal trajectory.

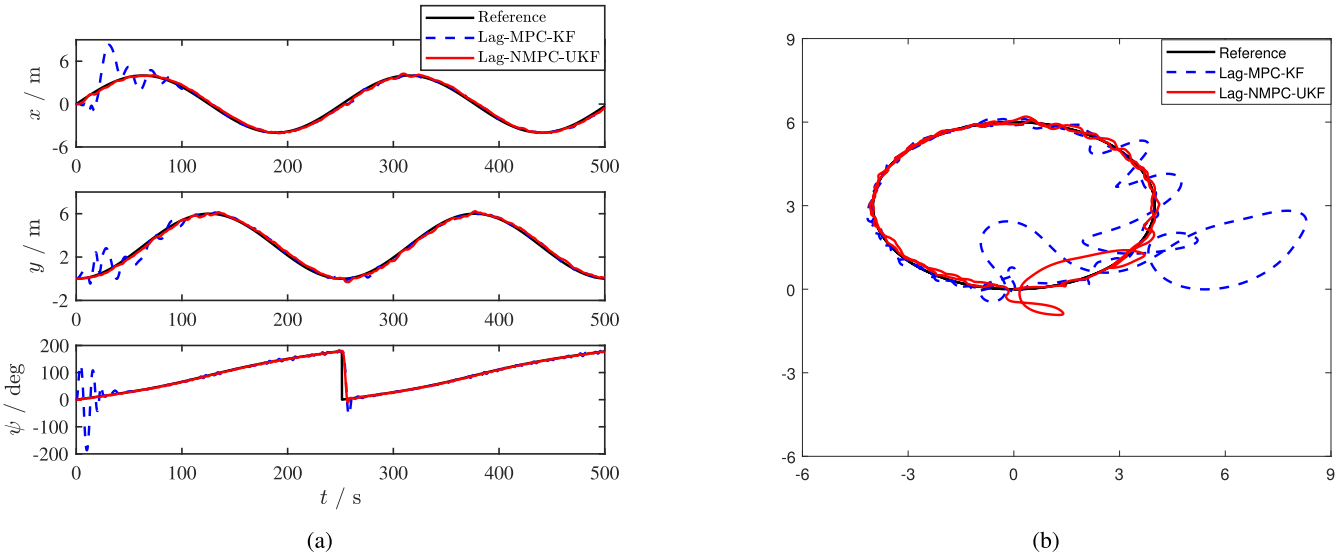

FIGURE 4. The simulation results of scenario 2 (trajectory tracking): (a) North-east position and heading (x, y, ψ); (b)Ship's horizontal trajectory.

A. SIMULATION SCENARIO AND PARAMETERS SETTING

In order to verify the control performance for different modes of the DP system, two scenarios are defined as follows for simulations. Scenario 1 simulates the setpoint regulation mode. It is the most basic mode of the DP system. In this mode, the DP ship is demanded to keep at a predefined position and heading or sail slowly from the initial position to another required position. In the simulation, the initial states, including the position, heading, and velocities of the ship is $\boldsymbol{x}(0)$=[0 m, 0 m, 0 deg, 0 m/s, 0 m/s, 0 deg/s]^T. The required position and heading are set as $\boldsymbol{\eta}_d$=[1 m, 0.5 m, 20 deg]^T. The reference input is set as $\boldsymbol{\eta}_r = \frac{1}{10s+1}\boldsymbol{\eta}_d$ to achieve a smooth control. Scenario 2 simulates the trajectory tracking mode. In this mode, the DP vessel is required to track a predefined smooth trajectory $\boldsymbol{\eta}_r$. In this paper, the reference trajectory is set as:

$$x_r(t) = 4\sin(0.025 * t)$$
$$y_r = 3 - 3 * \cos(0.025 * t), \qquad t \geq 0$$

The reference heading $\boldsymbol{\psi}_r(t)$ is choosen as the direction of the tangent vector along the path $(x_r(t), y_r(t))$. The disturbance is modelled as a first-order Markov process: $\dot{\boldsymbol{d}} = -\boldsymbol{T}_d^{-1}\boldsymbol{d} + \boldsymbol{R}_b\boldsymbol{\xi}$, with $\boldsymbol{T}_d = diag(100, 100, 100)$, $\boldsymbol{d}(0) = [0\ N, 0\ N, 0\ N \cdot m]^T$ and $\boldsymbol{R}_b = diag(0.1, 0.05, 0.025)$ in both scenarios.

The Laguerre functions were utilized together with the linear MPC algorithm for most applications for DP systems. Herein this scheme is expressed as Lag-LMPC.

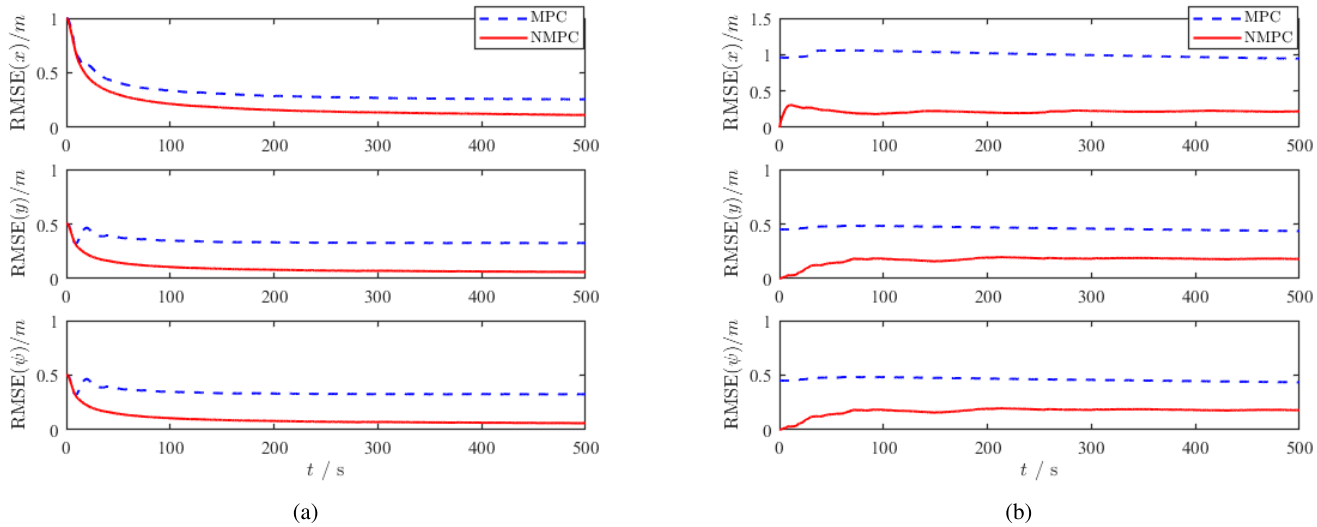

FIGURE 5. Position-heading root mean square error (RMSE) comparison of Lag-NMPC-UKF and Lag-MPC-KF:(a)scenario 1,(b)scenario 2.

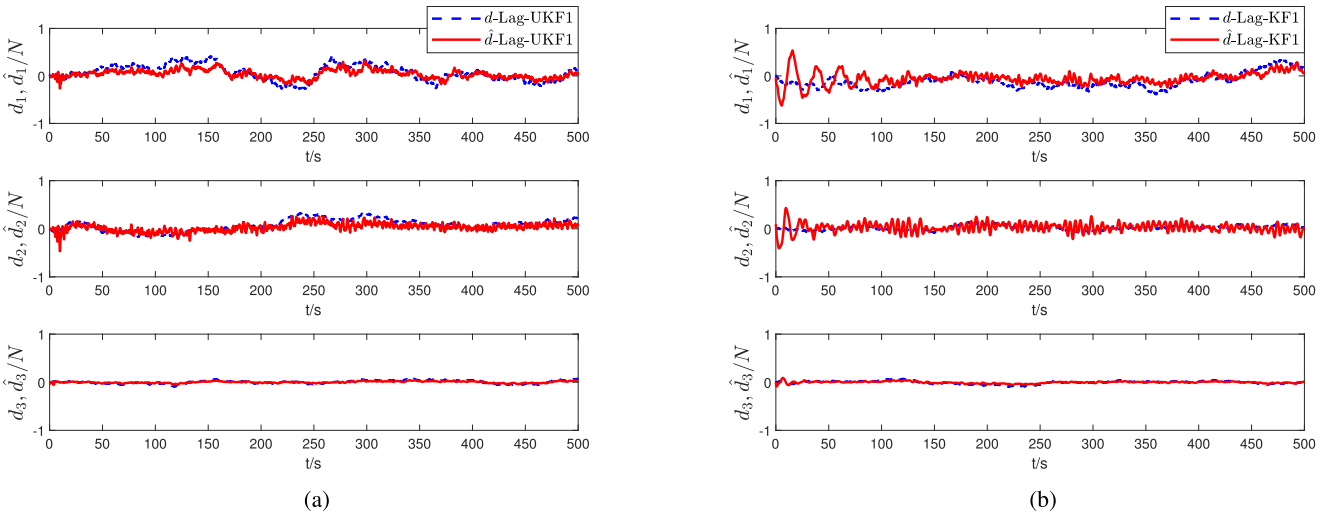

FIGURE 6. Results comparison between actual disturbances and their estimates for scenario1: (a) actual and estimated disturbance of UKF, (b) actual and estimated disturbance of KF.

In Lag-LMPC, assuming that the yaw rate is approximated to zero ($\dot{\psi} = r = 0$) and $\dot{R}(\psi) = 0$, the nonlinear DP model can be approximated to a linear state-space form, that the linear MPC together with the Kalman filtering (KF) method can be adopted for controller and state estimator design. To demonstrate the effectiveness of the proposed Lag-NMPC strategy, the Lag-LMPC strategy is also simulated. For the convenience of description, the two controller design methods are expressed as "Lag-MPC- KF" and "Lag-NMPC-UKF" in the following discussions.

In both two methodologies, parameter settings for the controller and the state estimator are identical. The sample time is $T_s = 0.1s$, the prediction horizon is $N_P = 50$, the scale factor and the number of terms are set as $\boldsymbol{a} = [0.5, 0.5, 0.5]^T$ and $\boldsymbol{N} = [10, 10, 10]^T$, and the weighting matrices $\boldsymbol{R}_L$ is a diagonal matrix $\boldsymbol{N}_{sum} \times \boldsymbol{N}_{sum}$ and $\boldsymbol{Q}_L = \boldsymbol{C}_a^T \boldsymbol{C}_a$, respectively. The parameters for UKF and KF estimator are set as: $\hat{\boldsymbol{\chi}}(0) = 0_{15\times 1}$, $\boldsymbol{P}(0) = \boldsymbol{I}_{15\times 15}$, $\boldsymbol{R} = diag\{0.02, 0.02, 0.001\}$, $\boldsymbol{Q} = diag\{0.09, 0.09, 0.001, 0.01, 0.01, 0.001, 0.01, 0.01, 0.001\}$.

B. RESULTS AND DISCUSSIONS

In order to verify the calculation efficiency of the designed controller, the calculation time for NMPC (and MPC) with (and without) the Laguerre function are listed in Table 2. It can be seen from Table 2 that compared with the algorithms without the Laguerre function in the setpoint regulation mode, the online calculation time for both MPC and NMPC with the Laguerre function are significantly reduced, which can well prove that the introduction of the Laguerre function can reduce the calculation complexity of the system. In addition, since NMPC needs to linearize the nonlinear model near the operating point at each time step when solving

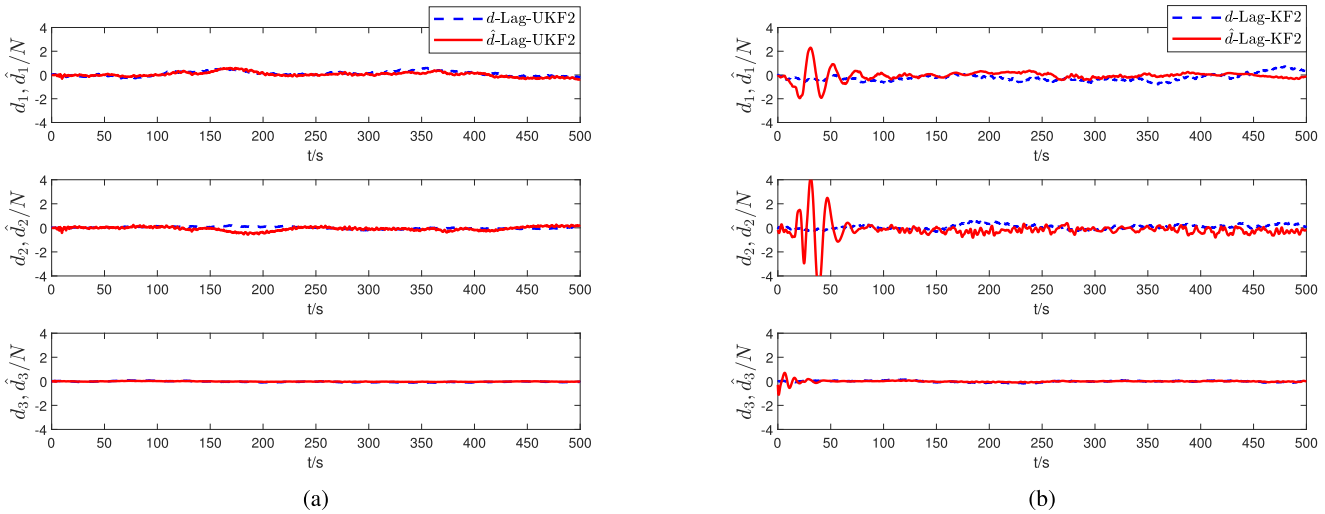

FIGURE 7. Results comparison between actual disturbances and their estimates for scenario 2: (a) actual and estimated disturbance of UKF, (b) actual and estimated disturbance of KF.

TABLE 2. Comparison of mean computation time in the setpoint regulation mode.

	NMPC	MPC
With Laguerre function	0.023s	0.013s
Without Laguerre function	0.044s	0.027s

TABLE 3. Comparison control error of Lag-NMPC-UKF and Lag-LMPC-KF.

average RMSE	setpoint regulation mode		trajectory tracking mode	
	Lag-NMPC	Lag-LMPC	Lag-NMPC	Lag-MPC
x /m	0.1086	0.2679	0.2124	0.9433
y /m	0.0579	0.3268	0.1770	0.4352
ψ /deg	0.0199	0.0295	0.2071	0.4212

the nonlinear optimization problem, the online calculation time of Lag-NMPC is higher than that of Lag-MPC, but the calculation time is significantly reduced compared with the traditional NMPC controller.

The simulation results of the two scenarios are shown in Figs 3–4. Among them, the simulation results of Lag-NMPC-UKF are represented by red solid lines, the results of Lag-MPC-KF are described by blue dotted lines, and solid black lines describe the reference trajectory. First, find the results of the setpoint regulation scenario in Fig. 3. Fig. 3(a) shows the change curve of ship position (x, y) and heading ψ. It can be seen from the figure that when the Lag-NMPC-UKF method is adopted, the ship position can better track the required position with a small tracking error. When the Lag-MPC-KF method is adopted, the position deviation is larger, but the heading tracking error is small. The control performance can also be seen from Fig. 3(b), which shows the ship's motion trajectory in the horizontal plane. Results demonstrate that the Lag-NMPC-UKF method has higher control accuracy in the setpoint regulation scenario. Fig. 4 shows the result comparisons of scenario 2. Fig. 4(a) and (b) indicate that the ship can precisely track the predefined trajectory by using the Lag-NMPC-UKF scheme, while when the Lag-MPC-KF scheme is adopted, there is a huge overshoot at the initial stage, and the ship deviates significantly from the predefined trajectory. Identical with the setpoint regulation scenario, the results verify the control efficiency of the proposed Lag-NMPC-UKF scheme. To quantitatively compare Lag-MPC-KF and Lag-NMPC-UKF, the following root mean square error (RMSE) was defined to evaluate the control accuracy:

$$\boldsymbol{RMSE} = \sqrt{\frac{1}{N_k}\sum_{k=1}^{N_k}(\boldsymbol{y} - \boldsymbol{\eta_r})}$$

where N_k is the sample time, $\boldsymbol{y}$ is the actual position and heading, $\boldsymbol{\eta_r}$ is the reference position and heading. Fig.5 shows the position-heading RMSE comparison results of Lag-MPC-KF and Lag-NMPC-UKF schemes in the two scenarios. In addition, the average RMSE values of the two control schemes in the simulation are listed in Table 3 for comparison. It can be seen from Fig.5 and Table 3 that the control error of the system when adopted the Lag-NMPC-UKF scheme is significantly smaller than the Lag-MPC-KF scheme. This further proves the feasibility and effectiveness of the proposed Lag-NMPC-UKF scheme. In addition, Figs. 6-7 shows the comparison curves of the real disturbance $\boldsymbol{d}$ and its estimated value $\hat{\boldsymbol{d}}$ under the two scenarios using UKF and KF, respectively. It can be seen from the figure that the estimated disturbances under the two scenarios can well reflect the real disturbances. Through comparison, it can be seen that when using UKF, the estimation error can be controlled in a small range. In contrast, when using KF, the disturbance estimates fluctuate obviously. It shows that the UKF algorithm performs better state estimation and filtering. Therefore, through the analysis of simulation results, we can conclude that the proposed lag-NMPC-UKF control scheme

has superior control performance and robustness for DP ships under unknown disturbances and input saturation.

V. CONCLUSION

In this paper, the NMPC controller is designed using Laguerre functions for dynamic positioning ships in the presence of input constraints and unknown disturbances. The use of Laguerre functions simplifies the NMPC design and reduces the number of parameters required in the optimization algorithm, which brings great flexibility to the design of the controller. The disturbance estimates obtained by UKF are utilized as the cancellation signal to eliminate the effects of disturbances and achieve robust offset-free control. In order to verify the superiority of the control performance of the designed Laguerre function-based NMPC (Lag-NMPC) scheme, two scenarios of setpoint regulation and trajectory tracking are simulated and compared with the performance of typical Laguerre function-based linear MPC (Lag-LMPC) scheme. Simulation results demonstrated the effectiveness, robustness and superiority of Lag-NMPC. The proposed Lag-NMPC scheme shows minor control variances and consequently contributes to less power consumption; furthermore, it provides a novel solution of extending the Laguerre function to the nonlinear system with constraints and unknown disturbances.

REFERENCES

[1] F. Wang, M. Lv, and F. Xu, "Design and implementation of a triple-redundant dynamic positioning control system for deepwater drilling rigs," *Appl. Ocean Res.*, vol. 57, pp. 140–151, Apr. 2016.

[2] T. I. Fossen, *Guidance and Control of Ocean Vehicles*, vol. 32, no. 8. Chichester, U.K.: Wiley, 1999, pp. 1235–1236.

[3] Å. Grøvlen and T. I. Fossen, "Nonlinear control of dynamic positioned ships using only position feedback: An observer backstepping approach," in *Proc. 35th IEEE Conf. Decis. Control*, vol. 3, Dec. 1996, pp. 3388–3393.

[4] K. Liang, X. Lin, Y. Chen, Y. Liu, Z. Liu, Z. Ma, and W. Zhang, "Robust adaptive neural networks control for dynamic positioning of ships with unknown saturation and time-delay," *Appl. Ocean Res.*, vol. 110, May 2021, Art. no. 102609.

[5] F. Deng, L.-J. Wang, and D.-M. Jiao, "Adaptive observer based backstepping controller design for dynamic ship positioning," *China Ocean Eng.*, vol. 31, no. 5, pp. 639–645, Oct. 2017.

[6] K. Liang, X. Lin, Y. Chen, J. Li, and F. Ding, "Adaptive sliding mode output feedback control for dynamic positioning ships with input saturation," *Ocean Eng.*, vol. 206, Jun. 2020, Art. no. 107245.

[7] Y. Wang, Y. Tuo, S. X. Yang, M. Biglarbegian, and M. Fu, "Reliability-based robust dynamic positioning for a turret-moored floating production storage and offloading vessel with unknown time-varying disturbances and input saturation," *ISA Trans.*, vol. 78, pp. 66–79, Jul. 2018.

[8] A. Afram and F. Janabi-Sharifi, "Theory and applications of HVAC control systems—A review of model predictive control (MPC)," *Building Environ.*, vol. 72, pp. 343–355, Feb. 2014.

[9] D. Q. Mayne, "Model predictive control: Recent developments and future promise," *Automatica*, vol. 50, no. 12, pp. 2967–2986, Aug. 2014.

[10] D. Q. Mayne, J. B. Rawlings, C. V. Rao, and P. O. M. Scokaert, "Constrained model predictive control: Stability and optimality," *Automatica*, vol. 36, no. 6, pp. 789–814, 2000.

[11] S.-R. Oh and J. Sun, "Path following of underactuated marine surface vessels using line-of-sight based model predictive control," *Ocean Eng.*, vol. 37, nos. 2–3, pp. 289–295, Feb. 2010.

[12] H. Zheng, R. R. Negenborn, and G. Lodewijks, "Trajectory tracking of autonomous vessels using model predictive control," *IFAC Proc. Volumes*, vol. 47, no. 3, pp. 8812–8818, 2014.

[13] X. Qian, Y. Yin, X. Zhang, X. Sun, and H. Shen, "Model predictive controller using Laguerre functions for dynamic positioning system," in *Proc. 35th Chin. Control Conf. (CCC)*, Jul. 2016, pp. 4436–4441.

[14] M. Jama, A. Wahyudie, and H. Noura, "Robust predictive control for heaving wave energy converters," *Control Eng. Pract.*, vol. 77, pp. 138–149, Aug. 2018.

[15] M. Ławryńczuk, "Nonlinear model predictive control for processes with complex dynamics: A parameterisation approach using Laguerre functions," *Int. J. Appl. Math. Comput. Sci.*, vol. 30, no. 1, pp. 35–46, 2020.

[16] E. A. Abioye, M. S. Z. Abidin, M. N. Aman, M. S. A. Mahmud, and S. Buyamin, "A model predictive controller for precision irrigation using discrete lagurre networks," *Comput. Electron. Agricult.*, vol. 181, Feb. 2021, Art. no. 105953.

[17] A. Bemporad, F. Borrelli, and M. Morari, "Model predictive control based on linear programming—The explicit solution," *IEEE Trans. Autom. Control*, vol. 47, no. 12, pp. 1974–1985, Dec. 2002.

[18] M. Liu, H. Wu, J. Wang, and C. Wang, "Non-minimal state space model predictive control using Laguerre functions for reference tracking," *Asian J. Control*, vol. 24, no. 1, pp. 205–216, Jan. 2022.

[19] J. A. Rossiter, L. Wang, and G. Valencia-Palomo, "Efficient algorithms for trading off feasibility and performance in predictive control," *Int. J. Control*, vol. 83, no. 4, pp. 789–797, Apr. 2010.

[20] L. Wang, *Model Predictive Control System Design and Implementation Using MATLAB*. Springer, 2009.

[21] G. Zhang, L. Gao, H. Yang, and L. Mei, "A novel method of model predictive control on permanent magnet synchronous machine with Laguerre functions," *Alexandria Eng. J.*, vol. 60, no. 6, pp. 5485–5494, Dec. 2021.

[22] J. Yuan, M. Zhu, X. Guo, and W. Lou, "Trajectory tracking control for a stratospheric airship subject to constraints and unknown disturbances," *IEEE Access*, vol. 8, pp. 31453–31470, 2020.

[23] M. Elsisi and M. A. Ebrahim, "Optimal design of low computational burden model predictive control based on SSDA towards autonomous vehicle under vision dynamics," *Int. J. Intell. Syst.*, vol. 36, no. 11, pp. 6968–6987, Nov. 2021.

[24] T. C. F. Pinheiro and A. S. Silveira, "Constrained discrete model predictive control of an arm-manipulator using Laguerre function," *Optim. Control Appl. Methods*, vol. 42, no. 1, pp. 160–179, Jan. 2021.

[25] A. J. Rashidi, B. Karimi, and A. Khodaparast, "A constrained predictive controller for AUV and computational optimization using Laguerre functions in unknown environments," *Int. J. Control, Autom. Syst.*, vol. 18, no. 3, pp. 753–767, Mar. 2020.

[26] A. Veksler, T. A. Johansen, F. Borrelli, and B. Realfsen, "Dynamic positioning with model predictive control," *IEEE Trans. Control Syst. Technol.*, vol. 24, no. 4, pp. 1340–1353, Jul. 2016.

[27] F. Deng, H.-L. Yang, L.-J. Wang, and W.-M. Yang, "UKF based nonlinear offset-free model predictive control for ship dynamic positioning under stochastic disturbances," *Int. J. Control, Autom. Syst.*, vol. 17, no. 12, pp. 3079–3090, Dec. 2019.

[28] J. El Hadef, S. Olaru, P. Rodriguez-Ayerbe, G. Colin, Y. Chamaillard, and V. Talon, "Nonlinear model predictive control of the air path of a turbocharged gasoline engine using Laguerre functions," in *Proc. 17th Int. Conf. Syst. Theory, Control Comput. (ICSTCC)*, Oct. 2013, pp. 193–200.

[29] J. Guo, Q. Peng, and J. Zhou, "Disturbance observer–based nonlinear model predictive control for air-breathing hypersonic vehicles," *J. Aerosp. Eng.*, vol. 32, no. 1, Jan. 2019, Art. no. 04018121.

[30] H. Yang, F. Deng, Y. He, D. Jiao, and Z. Han, "Robust nonlinear model predictive control for reference tracking of dynamic positioning ships based on nonlinear disturbance observer," *Ocean Eng.*, vol. 215, Nov. 2020, Art. no. 107885.

[31] Y. Xu, Y. Yuan, and D. Zhou, "The composite-disturbance-observer based stochastic model predictive control for spacecrafts under multi-source disturbances," *J. Franklin Inst.*, vol. 358, no. 15, pp. 7603–7627, Oct. 2021.

[32] C. Bai, Z. Yin, Y. Zhang, and J. Liu, "Robust predictive control for linear permanent magnet synchronous motor drives based on an augmented internal model disturbance observer," *IEEE Trans. Ind. Electron.*, vol. 69, no. 10, pp. 9771–9782, Oct. 2022.

[33] T. I. Fossen, *Handbook of Marine Craft Hydrodynamics and Motion Control*. Chichester U.K.: Wiley, 2011.

[34] R. Skjetne, T. I. Fossen, and P. V. Kokotović, "Adaptive maneuvering, with experiments, for a model ship in a marine control laboratory," *Automatica*, vol. 41, no. 2, pp. 289–298, Feb. 2005.

[35] S. J. Julier and J. K. Uhlmann, "New extension of the Kalman filter to nonlinear systems," *Proc. SPIE*, vol. 3068, pp. 182–193, Apr. 1997.

[36] Å. V. Fannemel, "Dynamic positioning by nonlinear model predictive control," Norwegian Univ. Sci. Technol., Trondheim, Norway, Tech. Rep., 2009.

XIUHUI HOU received the B.S. degree in mechanical design, manufacturing and automation from the Qingdao Institute of Technology, in 2018. She is currently pursuing the M.S. degree with the Qingdao University of Science and Technology. Her current research interest includes dynamic positioning.

FANG DENG received the B.S. degree in process equipment and control engineering from Sichuan University, China, in 2003, the M.S. degree in chemical machinery from Zhejiang University, in 2006, and the Ph.D. degree in mechanical design and theory from the Qingdao University of Science and Technology, in 2019. Her current research interests include nonlinear control and estimation, adaptive control, and application in motion control of marine crafts.

HUALIN YANG received the B.S. degree in mechanical design and manufacturing from the Shandong Institute of Light Industry, in 1998, the M.S. degree in mechanical manufacturing and automation from the Qingdao University of Science and Technology, in 2003, and the Ph.D. degree in chemical machinery from Zhejiang University, in 2006. His current research interests include intelligent manufacturing, mechanical design, control, and automation.

DUNJING YU received the B.S. degree in mechanical design, manufacturing and automation from the Shandong University of Science and Technology, China, in 2017. He is currently pursuing the M.S. degree with the Qingdao University of Science and Technology. His current research interest includes ship motion control.

HANLIN ZHANG received the B.S. degree in mechanical design, manufacturing and automation from the Qingdao University of Science and Technology, in 2021, where he is currently pursuing the M.S. degree. His current research interest includes ship nonlinear disturbance estimation.

BOYANG LI received the B.S. and M.S. degrees in marine engineering from Dalian Maritime University, in 1999 and 2006, respectively. His current research interests include ship energy saving and emission reduction technology.